

Thyristor-Based Resonant Current Controlled Switched Reluctance Generator for Distributed Generation

Ali Emadi[†], Yogesh P. Patel* and Babak Fahimi**

Abstract - This paper covers switched reluctance generator (SRG) and its comparison with induction and synchronous machines for distributed generation. The SRG is simple in design, robust in construction, and fault tolerant in operation; it can also withstand very high temperatures. However, the performance and cost of the SRG power electronics driver are highly affected by the topology and design of the converter. IGBT and MOSFET based converters are not suitable for very high power applications. This paper presents thyristor-based resonant converters which are superior candidates for very high power applications. Operations of the converters are analyzed and their characteristics and dynamics are determined in terms of the system parameters. The resonant converters are capable of handling high currents and voltages; these converters are highly efficient and reliable as well. Therefore, they are suitable for high power applications in the range of 1MW or larger for distributed generation.

Keywords: DC/AC inverter, Distributed generation, Induction machine, Power converters, Resonant converters, Switched reluctance generator, Synchronous machine

1. Introduction

There are many applications where switched reluctance machines (SRMs) offer distinct advantages over the conventional induction and synchronous machines. This is due to the simplified design, robust construction, fault tolerance operation, substantial saving in the operation and maintenance expenses, and tolerance to high temperature [1]-[8].

One of the main aspects of research in switched reluctance generators (SRGs) has been the converter design. The performance and the cost of the driver are highly affected by the topology of the converter. Almost all the power electronic converters, which have been proposed for SRMs in the literature [9]-[11], are based on IGBTs and MOSFETs. However, for very high power applications, IGBTs and MOSFETs are not suitable. MOSFETs with high voltage and high current capabilities are not even available. For IGBT-based converters, IGBTs need to be connected in parallel to be able to handle high currents. This considerably reduces efficiency and increases cost. Besides, maintaining balance current sharing between parallel IGBTs is of great concern. However, utilizing

thyristors at high power applications is feasible because of their high voltage and current capabilities as well as low cost. Yet, the main challenge in this work is that, to the best of our knowledge, thyristors have not been used for SRG applications. This is mainly because SRGs have traditionally been used for lower power applications where IGBTs and MOSFETs are available.

In this paper, special attention is given to justify the use of SRM as generator by comparing it with the induction and synchronous machines. In addition, novel thyristor-based resonant converters for high power SRGs are proposed. Each converter operation is analyzed and its characteristics and dynamics are determined in terms of the system parameters. The mathematical analyses are performed for each mode of operation. Resonant circuit parameters have also been designed. Both turn-on and turn-off of the switches occur at zero current. Therefore, the switching losses are reduced considerably. Active energy recovery into a high-voltage source is used to reduce the fall time of the phase current during commutation period. The proposed topologies have advantages like high efficiency and low stress on the switching devices. Therefore, they are suitable for high power generation in range of 1MW or larger [12].

This paper is organized as follows. Section II is the comparison of various machines. Section III focuses on SRG and includes the fundamentals of operation as well as the classic converter for SRGs. Section IV describes the proposed resonant converter. A quasi-resonant converter is

[†] Corresponding Author: Department of Electrical and Computer Engineering, Illinois Institute of Technology, Chicago, Illinois, USA. (emadi@iit.edu)

* Department of Electrical and Computer Engineering, Illinois Institute of Technology, Chicago, Illinois, USA. (patyog6@iit.edu)

** Department of Electrical and Computer Engineering, University of Texas at Arlington, Arlington, Texas, USA. (fahimi@uta.edu)

presented in Section V. Section VI deals with the comparison of the resonant and quasi-resonant converters. Finally, Section VII presents the conclusion.

2. Comparison of Various Machines

2.1 Machine Classification

If we consider the machines on the principle of how the torque is produced, they can be classified in two different classes. In the first category, which includes induction and synchronous machines, the torque is generated by interaction between the two magnetic fields: one on the rotor and one on the stator. These machines could be differentiated by the geometry used and different methods of generating the two fields, i.e., permanent magnets, energized windings, or induced currents. In the second category, which includes SRM, the rotation of the rotor is created by the tendency of the rotor to align itself with the excited stator poles. This is because when a stator winding is energized, a reluctance torque is produced as the rotor moves to its minimum reluctance position. As the first excited phase makes the rotor poles move to the aligned position, the next phase to be excited is chosen to be the most aligned stator poles with respect to the required position.

2.2 Synchronous Generator

In synchronous machines, armature winding is stationary and mounted on the stator. The field winding is rotating and mounted on the rotor. If we consider the synchronous machine as synchronous generator, then DC excitation is given to the field winding by the DC source, e.g., 125V or 250V. When the rotor rotates, the stator conductors are cut by the magnetic flux; hence, they have induced emf produced in them. The stator and rotor cores are made up of stampings. Two types of rotors are used in synchronous machines. One is salient pole type, which is used in low and medium speed synchronous machines. Such machines are characterized by their large diameters and short axial length. The other is smooth cylindrical type, which is used for steam turbines, which run at very high speeds. Such rotors are designed mostly for 2-pole or 4-pole turbo generators running at 3600 or 1800 rpm. In synchronous machines, there exists a definite relationship among rotational speed (N) of the rotor, the frequency (f) of the generated emf, and the number of poles (P).

$$f = \frac{PN}{120} \quad (1)$$

The main disadvantage of the synchronous generator is that it is operated at a constant speed to deliver electric power at particular frequency. Therefore, the gearbox and other speed regulating or governing systems are necessary to maintain the speed of the generator. The efficiency of the gearbox is very low. Therefore, the overall efficiency of the turbine generator system reduces considerably. In addition, the speed regulating system is very complicated, which, in term, results in higher cost of the system. The failure of a single phase or more leads to the machine out of synchronism with the supply system.

2.3 Induction Machine

In an induction machine, the windings are arranged on the stator in a sinusoidal distribution. There are two types of rotor: squirrel cage and wound rotor. When the stator windings are connected to an external alternating current power source, a magnetic field is set up in the airgap, which rotates at the synchronous speed. Magnetizing current must be supplied by the system to which it is connected. Operating mode of the machine as a motor or generator depends solely on its speed. For the generation mode of operation, the rotor is driven by a prime mover at a speed slightly above the synchronous speed. The slip under this condition is considered to be negative and power is delivered from the mechanical prime mover to the supply line. Induction generators have been widely utilized for the electricity generation such as wind power. The main limitation of the induction generator is lack of control of the generator terminal voltage and frequency under varying stochastic wind [1]-[3]. In addition, when short-circuited, the generator delivers little or no sustained power because its excitation quickly becomes zero. The other disadvantage is that it cannot operate as an isolated power source. It must be connected to a power system capable of supplying the magnetizing current required to establish the magnetic field across the airgap. This tends to lower the power factor of the system and is usually compensated by shunt capacitors. Theoretically, the induction generator could operate as an isolated system with the magnetizing current supplied by the capacitors connected to the system; but, it is difficult to maintain the generator terminal voltage constant with changing load. In general, the induction generator has a lower efficiency than the comparably rated synchronous generator.

2.4 Switched Reluctance Machine

SRMs have the simplest mechanical structure compared with the induction and synchronous machines, making them one of the most interesting from the economic point of view. In SRM, the phase windings are only located on

the stator; the rotor is only made with steel laminations. There is no winding or permanent magnet on the rotor reducing the cost of the construction and increasing the thermal limit of the machine compared to the induction and synchronous machines. The torque produced by one phase of SRM at any rotor position is given by the equation below.

$$T = \frac{1}{2} i^2 \frac{dL}{d\theta} \quad (2)$$

The positive or negative sign of the current does not affect the torque, as torque is proportional to the square of the current. Torque is related to the slope of the inductance. Therefore, phase excitation during the positive slope of the inductance gives motoring mode and phase excitation during the negative slope of the inductance gives generating mode. This means that a single machine can be operated as a motor as well as a generator. SRG can operate over a wide range of speed eliminating the requirement of gearbox and speed governing systems, which provide the cost effective and simplified solution instead of using the synchronous generators. For SRG, phase windings are electrically separated from each other. Therefore, fault on one phase does not alter the operation of the other phases. The freedom to choose any number of phases is an inherent characteristic of SRG leading to high reliability of operation compared to the induction and synchronous generators. Furthermore, the SRG can work as an isolated power source with the separate excitation source for the phase windings. In most of the cases, the SRG system generates its own separate excitation, which overcomes the difficulty arises in the case of the induction generators. Fig. 1 shows the comparative study of different types of machine used for power generation.

3. Switched Reluctance Generator

3.1 Fundamentals

The switched reluctance generators convert the mechanical energy to the electrical energy by the virtue of proper synchronization of phase current with the rotor position. The torque production in SRG is the same as in the SRM. During generation, SRG produces the negative torque that trying to oppose the rotation of the rotor, thus, extracting energy from the prime mover. In SRG, it is essential to provide proper excitation to the phase windings to support continuous energy conversion. The ideal inductance profile, phase current, and torque for the SRG are depicted in Fig. 2.

The torque speed characteristic of the SRG is almost the

same as the SRM. During the constant torque region, the hysteresis control technique is used, as in SRM, to generate the electricity. The main difference is that, we need to shift the reference position by π / N_r . For both SRG and SRM, base speed is the speed at which phase currents are nominally constant without the need for the current regulation. Base speed can be taken to be the speed where the phase back-emf balances the source voltage and resistive drop. The base speed in the SRG is slightly higher than the SRM due to the different sign on the resistive drop. If the speed of the prime mover increases beyond the base speed, the phase current of the SRG is the mirror image of the SRM around the align rotor position (see Fig. 3). The main difference between the SRG and SRM is the effect of the motional back-emf [3], [4]. The motional back-emf in SRM decreases the phase current. The maximum phase current is determined by the turn-on angle only. Therefore, by advancing the turn-on angle, we can control the torque production. In SRG, the phase current is increased even after a turn-off command is issued. Due to the high-speed nature of the SRG, this might be an excessive and unexpected overcurrent during the turn-off process.

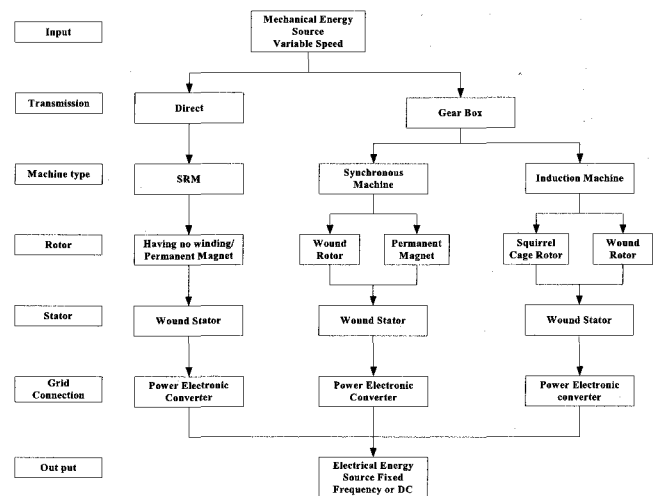


Fig. 1. Comparative study of different machines.

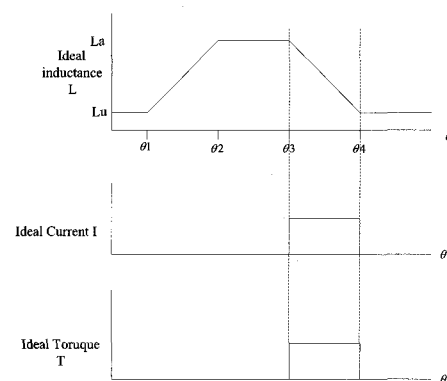


Fig. 2. Ideal inductance, current, and torque waveforms for SRG.

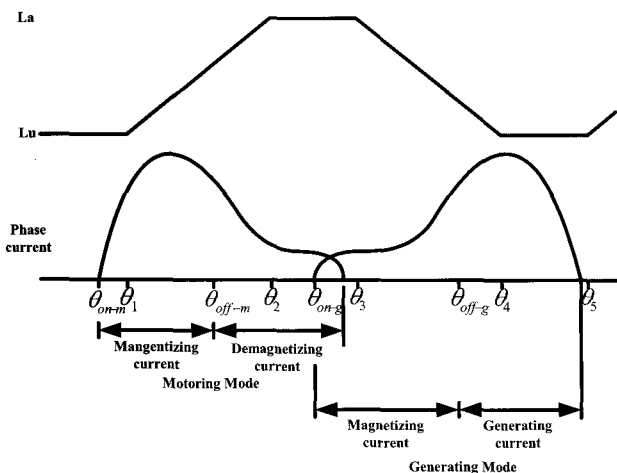


Fig. 3. Phase current during motoring and generating modes.

3.2 Classic Converter

For the low-power applications, the classic converter is the good candidate to drive SRGs [5]. Fig. 4 shows the SRG with the classic converter. MOSFETs or IGBTs are incorporated in the classic converter. The machine draws energy from the bus while switches are on and returns energy through the diodes when the switches are off. The generator obtains its excitation from the same bus that it generates into. Let's consider the square wave mode of operation; each IGBT switch turns on and off only once per cycle. This mode of operation is limited to the higher machine speeds, where the back-emf of the machine is comparable to or higher than the dc output voltage. At a given bus voltage, a certain amount of power and, thus, average generated current will be produced. Consider next a small perturbation where the bus voltage increases slightly. As the bus voltage increases, the machine excitations will increase, which, in turn, the generated current increases. This tends to increase the bus voltage further. Thus, there is a potential for instability. Furthermore, if there is a short circuit at the output of the SRG, it always exceeds the generators maximum loading capability and brings the voltage at the output of the SRG to zero. Even if a fuse is blown to disconnect the short circuit, the SRG does not recover its operation.

Providing a separate bus to excite the generator as shown in Fig. 5 can eliminate this problem. It is possible to provide excitation through the multiple dc buses [6]-[8]. These multiple buses can be connected to gather as shown in Fig. 4 with help of diode to provide necessary power to the excitation bus. The battery with diode provides the excitation during starting. Afterward, the other excitation source provides the necessary power. This excitation source can be charged though the energy generated by the SRG. The excitation source provides around 30% of the

power going to the load at the rated load. During each generating cycle, the phase winding is totally demagnetized requiring a large amount of excitation power. For the high power applications, one cannot use classic converter with MOSFETs or IGBTs.

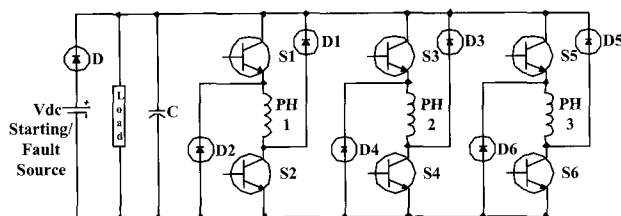


Fig. 4. Self-excited SRG.

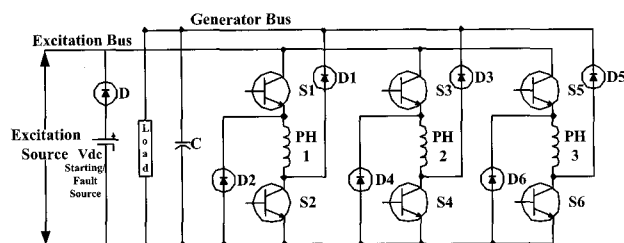


Fig. 5. Separate excitation bus for SRG.

4. Thyristor-Based Resonant Current Controlled Converter for SRG

The circuit for the thyristor-based resonant current controlled converter is shown in Fig. 6. The LC resonant circuit is connected in series with each resonant switch and in parallel with each machine phase winding. Auxiliary circuits are added to modify the converter configuration according to the operating modes, which are discussed in previous section. This auxiliary circuit is nothing but a Buck converter made up from L_d , D_d , S , and C_d . The pulse-width modulation (PWM) or frequency modulation (FM) scheme can be used to regulate the motor winding current. This in turn controls the output (electromagnetic torque or DC link voltage) at the desired value. The thyristor switching occurs at zero current, which minimizes switching losses. During the commutation period, the current in the off-going phase must be reduced to zero as fast as possible.

We assume that initially all the thyristors and diodes are off. The circuit operation can be divided into five different operating modes, similar to the motoring mode of operation [13]. The equivalent single-phase circuit is shown in Fig. 7.

In mode 1, a gating signal is applied to thyristor S2. The DC link voltage is supplying the magnetizing current to the machine phase winding. For the mathematical analysis of

different modes of operation, the phase current can be derived as [14], [15],

$$I_{m1}(t) = \frac{V_{dc} - E_b}{R} \left(1 - e^{-\frac{t}{\tau}}\right) + i_{m1}(0) \left(e^{-\frac{t}{\tau}}\right) \quad (3a)$$

$$\tau = \frac{L_{m1}(\theta)}{R} \quad (3b)$$

$$R = R_{ph} + R_T$$

R_T is the resistance of the thyristor S2. τ is the time constant of the circuit. The time constant is assumed to be constant in order to simplify the analysis. $i_{m1}(0)$ is the initial phase current.

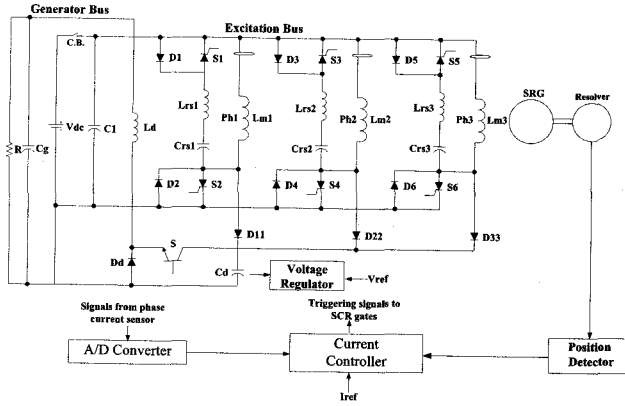


Fig. 6. Resonant converter for SRG with control circuit.

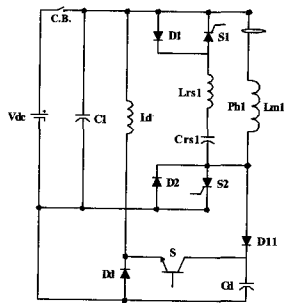


Fig. 7. Equivalent single-phase circuit of the resonant converter.

When S2 is triggered, a fast resonance occurs having the frequency given by,

$$f_{fr} = \frac{1}{2\pi\sqrt{L_{rs1}C_{rs1}}} \quad (4)$$

This charges C_{rs1} to $2V_{dc}$ through the loop D1, Lr1, S2, and V_{dc} . The equivalent circuit equations can be given as,

$$I_{m1}(t) = \frac{V_{dc} - E_b}{R} \left(1 - e^{-\frac{t}{\tau}}\right) + i_{m1}(0) \left(e^{-\frac{t}{\tau}}\right) \quad (5)$$

$$V_{dc} = L_{rs1} \frac{dI_{r1}}{dt} + V_{crs1} \quad (6)$$

$$V_{crs1} = \frac{1}{C_{rs1}} \int I_{r1} dt \quad (7)$$

However, in the simulations, we consider that phase winding current I_{m1} increases linearly with time having slope of V_{dc}/L_{m1} . Therefore, the equation for the phase current is given by,

$$I_{m1} = \frac{1}{L_{m1}} \int V_{dc} dt \quad (8)$$

In mode 2, when C_{rs1} is charged to $2V_{dc}$, the phase winding current reaches the reference value I_{ref} . This is the end of mode 2. The equivalent circuit equation can be given as,

$$I_{m1}(t) = \frac{V_{dc} - E_b}{R} \left(1 - e^{-\frac{t}{\tau}}\right) + i_{m1}(0) \left(e^{-\frac{t}{\tau}}\right) \quad (9)$$

In mode 3, when the phase winding current reaches its reference value I_{ref} , thyristor S1 is triggered. This causes a fast resonance having frequency given by $f_{fr} = \frac{1}{2\pi\sqrt{L_{rs1}C_{rs1}}}$.

The resonant current flows in counter clockwise direction through the loop L_{rs1} , S1, V_{dc} , S2, and C_{rs1} . Therefore, C_{rs1} is charged in the negative direction. The resonant current I_{r1} reduces the current through S2 to zero and then D2 conducts. After that, I_{r1} reaches its peak value of $-V_{dc}\sqrt{\frac{C_{rs1}}{L_{rs1}}}$, and then begins to decrease in magnitude.

When the negative I_{r1} equals to I_{m1} , S2 and D2 are opened. The circuit turn-off time is $t_0 + t_c$. At time $t_0 + t_c$, the phase current reaches its peak value. The equivalent circuit equations are given by,

$$I_{m1\max} = I_{m1}(t_0 + t_1) = \frac{V_{dc} - E_b}{R} \left(1 - e^{-\frac{t}{\tau}}\right) + I_{ref} \left(e^{-\frac{t}{\tau}}\right) \quad (10)$$

$$V_{dc} = L_{rs1} \frac{dI_{r1}}{dt} + V_{crs1} \quad (11)$$

$$V_{crs1} = \frac{1}{C_{rs1}} \int I_{r1} dt \quad (12)$$

In mode 4, only S1 is on. The phase current I_{m1} flows through the loop S1, L_{m1} , C_{rs1} , and L_{rs1} . This causes a slow resonance because there are two inductances added together. The frequency of the slow resonance is given by,

$$f_{sr} = \frac{1}{2\pi\sqrt{(L_{m1} + L_{rs1}) + C_{rs1}}} \quad (13)$$

This charges C_{rs1} in the negative direction. When C_{rs1} is charged negatively to the value $V_{dc} + |-V_{crs1}| \geq V_{cd} = 2V_{dc}$, where V_{cd} is the voltage across capacitor C_d , then D11 starts to conduct ending mode 4. We already noted that capacitor C_d had been charged to $2V_{dc}$. The circuit equations can be given as,

$$V_{cr1} + L_{m1} \frac{dI_{m1}}{dt} + L_{r1} \frac{dI_{r1}}{dt} = 0 \quad (14)$$

$$V_{crs1} = \frac{1}{C_{rs1}} \int I_{r1} dt \quad (15)$$

$$I_{m1} = -I_{r1} \quad (16)$$

In mode 5, there are two subsections. In the first part, L_{m1} and L_{rs1} are charging C_{rs1} in the negative direction until I_{r1} reduces to zero. When I_{r1} reaches its zero value, C_{rs1} is charged to its maximum value in the negative direction. Now, D11 conducts and S1 is off. I_{r1} reaches the maximum value of $V_{dc} \sqrt{\frac{(C_{rs1} + C_d)}{L_{rs1}}}$. D11 conducts as long as

$I_{m1} + I_{r1} > 0$. The phase winding I_{m1} then reduces to the desired value either only a few percentage below the reference value I_{ref} , if the conduction period continues or to zero when the phase current is turned off. For low speed operation, we need to define the tolerance limit above and below the reference value. Assume that the maximum deviation from reference current is 10% of the reference current. Therefore, the minimum phase current for the current control hysteresis method is as follows,

$$I_{m1 \min}(t) = 0.9I_{ref} \quad (17)$$

The rate of decrease of phase winding current depends upon the maximum value it attends previously.

$$I_{m1}(t) = \frac{V_{dc} - V_{cd} - E_b}{R} \left(1 - e^{-\frac{t}{\tau}}\right) + I_{m1 \max} \left(e^{-\frac{t}{\tau}}\right) \quad (18)$$

When $I_{m1}(t) = I_{m1 \min}$, thyristor S2 is triggered. Therefore, the cycle is repeated until period of conduction

is not complete. Once the period of phase conduction is about to complete, S2 is no longer triggered. And $I_{m1}(t)$ is allowed to decrease down to the zero value; during this time, it charges the dump capacitor C_d . The equivalent circuit equations are given as follows,

$$V_{dc} - V_{cd} = L_{rs1} \frac{dI_{rs1}}{dt} + V_{crs1} \quad (19)$$

$$V_{crs1} = \frac{1}{C_{rs1}} \int I_{r1} dt \quad (20)$$

For reliable operation of the circuit, V_{cd} must be equal to $2V_{dc}$. This condition is fulfilling to some extent by using a large capacitor. In that case, the changes in the capacitor voltage due to the discharge of the trapped energy of the phase winding will be small. One can keep this voltage constant by mean of PWM control of the IGBT. The following are equations describing the modes of operations.

$$V_{dc} + R_d I_{rec} + L_d \frac{dI_{rec}}{dt} = \begin{cases} V_{cd} & 0 < t < d_1 T \\ 0 & d_1 T < t < T \end{cases} \quad (21)$$

$$I_{rec}(t) = \frac{V_{cd} - V_{dc}}{R_d} \left(1 - e^{-\frac{t}{\tau}}\right) + I_{rec}(0) \left(e^{-\frac{t}{\tau}}\right) \quad 0 < t < d_1 T \quad (22)$$

$$\tau_r = \frac{L_d}{R_d} \quad (23)$$

R_d is the resistance of the recovery inductor and its inductance is L_d . The equation of the current in inductor when IGBT is off is given by,

$$I_{rec}(t) = \frac{-V_{dc}}{R_d} \left(1 - e^{-\frac{t}{\tau}}\right) + I_{rec}(0) \left(e^{-\frac{t}{\tau}}\right) \quad d_1 T < t < T \quad (24)$$

$$t' = (1 - d_1)T \quad (25)$$

The duty cycle, d_1 is variable and determined by the feedback circuit to keep the voltage across C_d constant, which is equal to $2V_{dc}$. The waveforms for the above modes of operations are given in Fig. 8.

Simulations of the thyristor based resonant current controlled converter have been carried out in PSIM software. In these simulations, we have assumed that the phase winding inductance is constant and current through the inductance varies linearly. The current through the phase winding, the voltage across the phase winding, the current through the resonant circuit, and the voltage across the resonant capacitor are shown in Fig. 9. The zoom in

waveforms is shown in Fig. 10. The waveforms are approximately the same as we derived from the mathematical analysis. The voltage across the dump capacitor, the current through the IGBT, the current through the diode D_d , and the current through the inductance L_d are shown in Fig. 11. Phase inductance is $L_{m1}=0.5\text{mH}$; resonant inductance is $L_{rs1}=5.4\mu\text{H}$; resonant capacitor is $C_{rs1}=12\mu\text{F}$; dump capacitor is $C_d=20\text{mF}$; dump inductor is $L_d=0.1\text{mH}$; and capacitor is $C_1=10\mu\text{F}$.

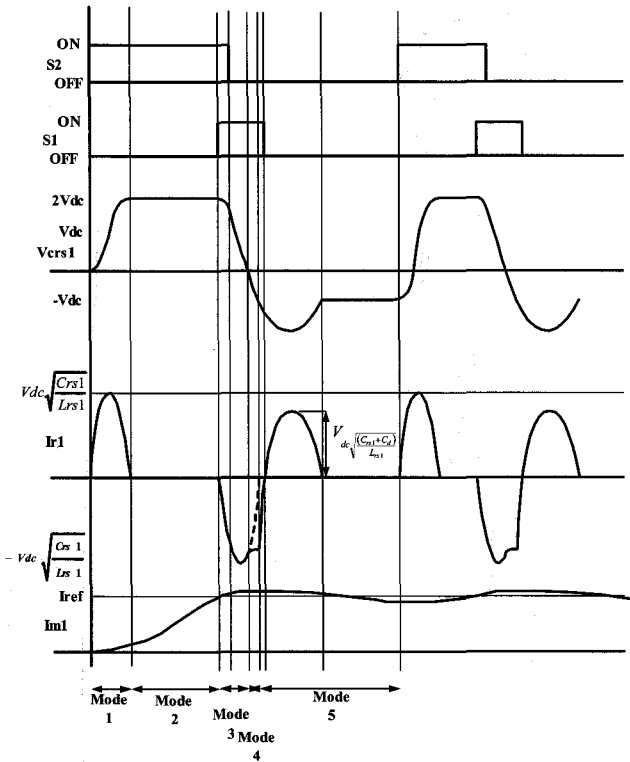


Fig. 8. Waveforms for the resonant converter.

Simulations of the resonant current controlled converter for hysteresis current control operation have also been carried out. The current through the phase winding, the voltage across the phase winding, the current through the resonant inductor, and the voltage across the resonant capacitor is shown in Fig. 12. The enlarged waveforms are shown in Fig. 13. The current through switches S_1 and S_2 and diodes D_1 and D_2 are shown in Fig. 14. Phase inductance is $L_{m1}=0.5\text{mH}$; resonant inductance is $L_{rs1}=5.4\mu\text{H}$; resonant capacitor is $C_{rs1}=12\mu\text{F}$; dump capacitor is $C_d=20\text{mF}$; dump inductor is $L_d=0.1\text{mH}$; and capacitor is $C_1=10\mu\text{F}$.

The thyristors are used as power switches, which can withstand high voltages and currents compared to MOSFETs and IGBTs. Therefore, the converters are suitable for high power applications. The large dump capacitor is used for the energy recovery during the generating mode, which leads to a reduction in fall time of

the phase current during the commutation period. The thyristors are turned on and off at the zero current. Therefore, the switching losses are reduced and system efficiency is improved. Variable structure approach is used in order to optimize the converter performance versus the operating conditions. In addition, each phase is independent of each other.

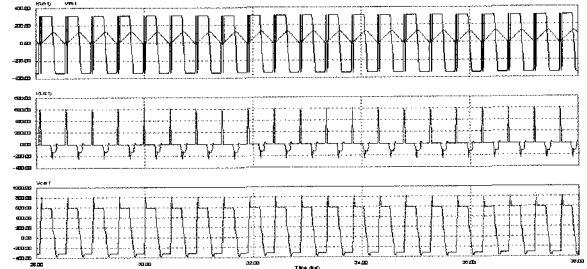


Fig. 9. I_{m1} , V_{ph1} , I_{rs1} , and V_{crs1} of the resonant current controlled converter.



Fig. 10. Enlarged waveforms of I_{m1} , V_{ph1} , I_{rs1} , and V_{crs1} .

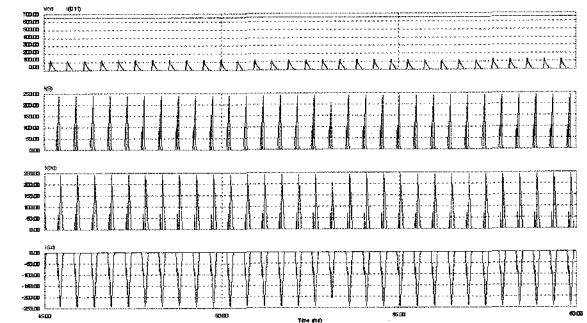


Fig. 11. V_{cd} , and currents through D_{11} , S , and D_d .

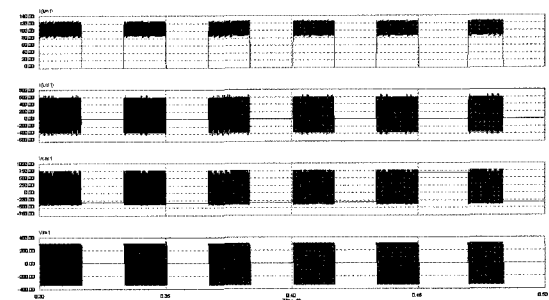


Fig. 12. I_{m1} , V_{crs1} , I_{rs1} , and V_{ph1} of the resonant current controlled converter.

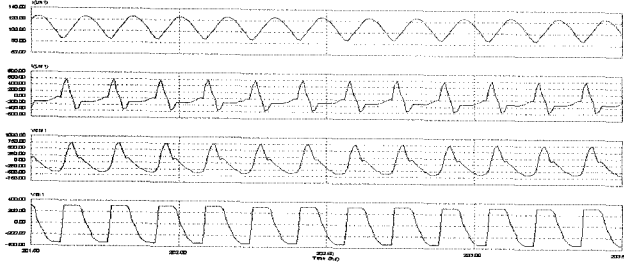


Fig. 13. Enlarged waveforms of I_{ph1} , I_{Lrs1} , V_{crs1} , and V_{ph1} .

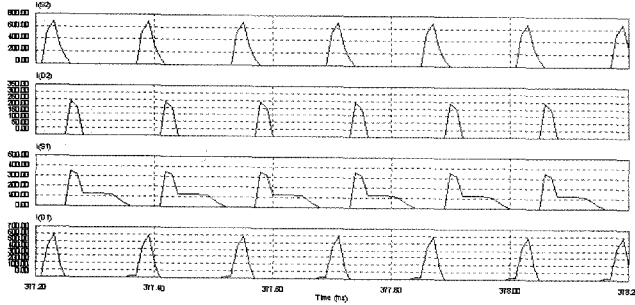


Fig. 14. Waveforms of currents through S1, S2, D1, and D2.

5. Quasi-Resonant SRG Converter

The operation of the proposed quasi-resonant converter for SRG can be de divided into two distinct periods: (1) active and (2) commutation. In active period, the current is conducted in one phase, the other phases being cut off. During commutation period, current in the off going phase is reduced to zero and current in on going phase has to build up from zero. For the low speed application, the current in the machine phase winding must be regulated by the pulse width or frequency modulation. In these schemes, the thyristors are turned on and off at high frequency. The zero current switching can be applied during this period to eliminate turn off losses. The resonant circuit is used to do this job. During the commutation period, off going phase

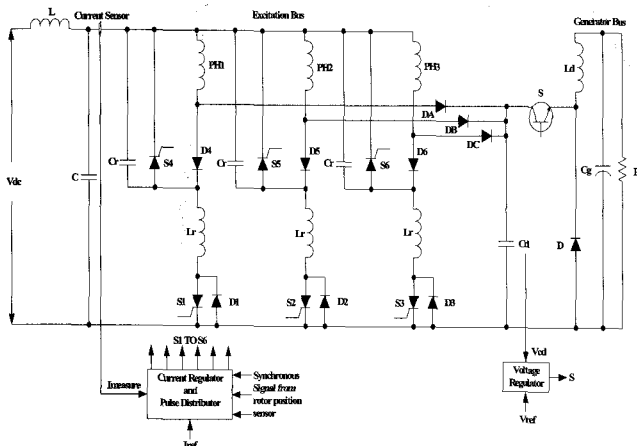


Fig. 15. Quasi-resonant current controlled converter for SRG.

energy is dump into the large capacitor. This leads to reduction in the commutation interval. The converter circuit is shown in Fig. 15. There are three resonant switches, each of them formed by a thyristor in parallel with a diode and LC resonant circuit. The single-phase equivalent circuit is also shown in Fig. 16.

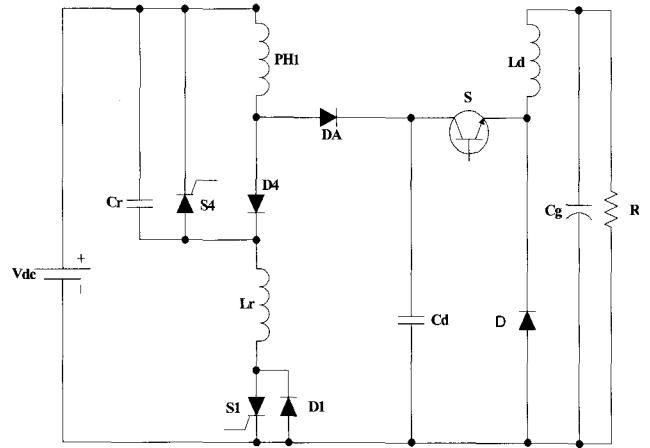


Fig. 16. Single-phase equivalent circuit of quasi-resonant converter.

5.1 Active Phase Period

The active phase period equivalent circuit is shown in Fig. 17. The current regulator regulates the phase current during the active phase period, which controls the operating frequency of the resonant switches. We assume that, during the active phase period, the currents in other phases are zero. The on-state voltages of the diodes and thyristors are negligible.

During the active phase, the phase winding is represented by an equivalent circuit consisting of an inductance $L_a(\theta)$, a resistance R_a , and a back-emf E_a , which is proportional to current I_a , machine speed, and rate of change of inductance with rotor position.

$$E_a = \left[\frac{dL_a(\theta)}{d\theta} \omega \right] I_a \quad (26)$$

From the equation (26), one can represent back-emf by an equivalent resistor of value $\left(\frac{dL_a}{d\theta} \omega \right)$. The equivalent circuit consists of an inductance $L_a(\theta)$ in series with resistance $R_x = R_a + \left(\frac{dL_a}{d\theta} \omega \right)$ shown in Fig. 18. The

machine phase winding carries current I_o ; therefore, it can be represented by a current source equal to I_o . The different operating modes during the active phase period are as the following.

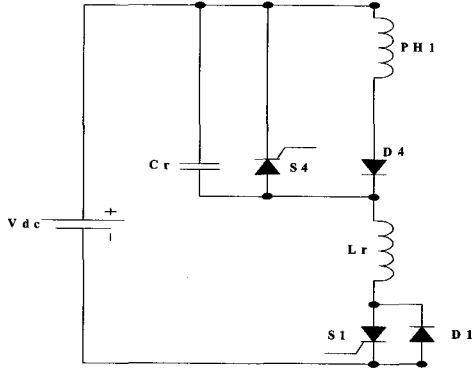


Fig. 17. Circuit configuration of quasi-resonant during active phase period.

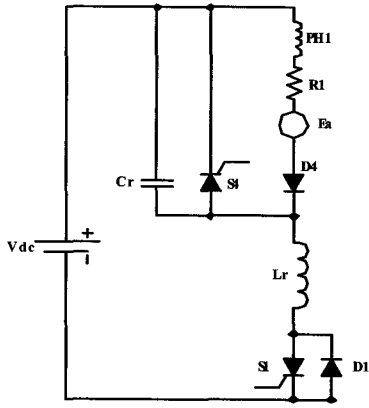


Fig. 18. Equivalent circuit during active period of quasi-resonant converter.

Mode 1: Assume that initially switch S1 and diode D1 are off. The machine phase current I_o is circulating through free wheeling thyristor S4. Now S1 is turned on. The current through L_r increases linearly with a slope equal to V_{dc}/L_r . When the current I_l reaches to I_o , switch S4 turns off and resonance between L_r and C_r begins. The equivalent circuit equations are as follows.

$$iL = \frac{1}{L_r} \int V_{dc} dt \quad (27)$$

$$V_{dc} = L_r \frac{diL}{dt} + V_{cr} \quad (28)$$

$$V_{cr} = \frac{1}{C_r} \int iL dt \quad (29)$$

The duration of mode 1 can be calculated as

$$t_1 = L_r \frac{I_o}{V_{dc}} \quad (30)$$

Mode 2: During this mode, S1 is conducting and current I_L and Voltage V_{cr} vary sinusoidally. The frequency

of the resonant frequency is given by the equation $f = 1/2\pi\sqrt{L_r C_r}$. Equivalent circuit equations are given as follows.

$$iL = \frac{1}{L_r} \int V_{dc} dt \quad (31)$$

$$V_{dc} = L_r \frac{diL}{dt} + V_{cr} \quad (32)$$

$$V_{cr} = \frac{1}{C_r} \int iL dt \quad (33)$$

When I_L goes zero, thyristor S1 turns off and diode D1 starts conducting. The time duration of this stage can be calculated as

$$t_2 = \frac{\tau}{2} + t_2' \Big|_{iL=0} \quad (34)$$

where τ is the time period of one cycle of the resonance.

$$t_2 = \frac{\pi}{\omega} + \frac{\sin^{-1}\left(\frac{I_o}{V_{dc}} \sqrt{\frac{L_r}{C_r}}\right)}{\omega} \quad (35)$$

$$t_2 = \sqrt{L_r C_r} \left(\pi + \sin^{-1}\left(\frac{I_o}{V_{dc}} \sqrt{\frac{L_r}{C_r}}\right) \right) \quad (36)$$

Mode 3: Diode D1 conducts current I_L until it reaches zero again. The circuit equations remain the same. The time duration for the mode is given by

$$t_3 = \frac{\tau}{2} + 2 \cdot t_2' \quad (37)$$

$$t_3 = \sqrt{L_r C_r} \left(\pi - 2 \sin^{-1}\left(\frac{I_o}{V_{dc}} \sqrt{\frac{L_r}{C_r}}\right) \right) \quad (38)$$

In mode 3, negative voltage is applied across thyristor S1 until t_3 . To ensure reliable turnoff, t_3 should be greater than the turnoff time t_q of the thyristor S1.

Mode 4: In this mode, the capacitor is discharged by the current source I_o . When the capacitor voltage is zero, the auxiliary switch S4 is turned on to provide a continuous path for the current source I_o . Then, the freewheeling period begins. For the low speed, the SRG is operated by hysteresis current control technique. Therefore, one needs to repeat the above modes. For the high speed, SRG is operated in single pulse mode. Therefore, the commutation period starts right after mode 4. The duration of mode 4 is

given by

$$t_4 = \frac{V_{dc}}{I_o} C_r \left[1 - \sqrt{1 - \frac{L_r}{C_r} \left(\frac{I_o}{V_{dc}} \right)^2} \right] \quad (39)$$

The maximum I_L can be calculated as

$$I_{L_{max}} = I_o + \frac{V_{dc}}{\sqrt{\frac{L_r}{C_r}}} \quad (40)$$

The waveforms for phase A of the quasi-resonant converter during the active phase period are shown in Fig. 19.

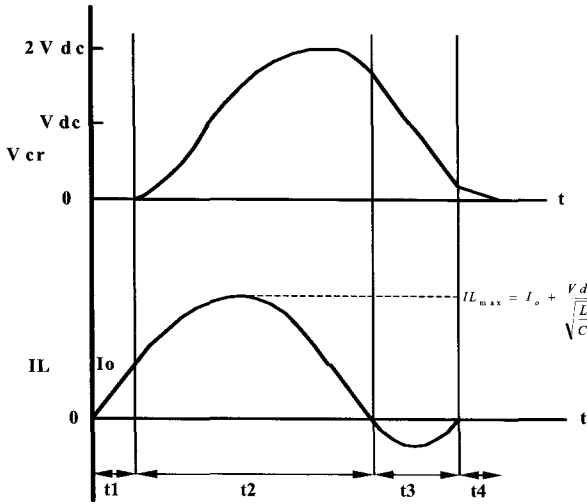


Fig. 19. Waveforms of phase A during active phase period.

5.2 Commutation Period

For the SRG at low-speed operation, the commutation is relatively easy compared to the high-speed operation due to the higher energy level involved. For the high-speed operation of SRG, the phase current goes through the peak value after the turnoff. The turn off energy at high-speed operation is $0.5LI_{peak}^2$, which is very high compared to the low speed operation ($0.5LI_a^2$). Dumping this energy into a capacitor can accelerate the low-speed and high-speed operations of the SRG during turnoff. The capacitor voltage must be maintained at a high and safe value. A chopper driven by a voltage regulator can do this. During the turnoff time, the triggering signal for auxiliary thyristor S4 is inhibited. Therefore, there is no freewheeling path through S4. A small part of the energy stored in the phase winding is recovered into C_r . The remaining stored energy is dumped into the capacitor C_d . The equivalent circuit for the commutation period is shown in Fig. 20. The turnoff operation can be divided into two modes.

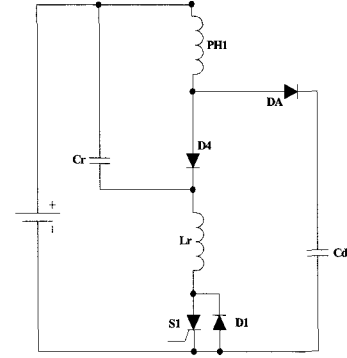


Fig. 20. Circuit during commutation period of quasi-resonant converter.

Mode 1: During this mode, the phase A winding current flow through D4 to charge C_r in negative direction. When the capacitor voltage attains value $|V_{dc} + V_{cr}| \geq V_{cd}$, the diode DA begins to conduct and D4 stops conducting. The duration of this mode is given by equation as

$$t_{f-1} = C_r \frac{V_{cd} - V_{dc}}{I_o} \quad (41)$$

Mode 2: The current in phase A decreases exponentially with time constant equal to $R_x = R_a + \left(\frac{dL_a}{d\theta} \omega \right)$. This time constant is supposed to be a constant in order to simplify the analysis. Current I_a during this stage can be determined as follows.

$$I_a = \frac{V_{dc} - V_{cd}}{R_x} + \left(I_o + \frac{V_{cd} - V_{dc}}{R_x} \right) e^{-\left[\frac{R_x}{L} \right] t} \quad (42)$$

At the end of mode 2, $I_a = 0$. The duration of this stage is equal to

$$t_{f-2} = \frac{L}{R_x} \ln \left(1 + \frac{R_x I_o}{V_{cd} - V_{dc}} \right) \quad (43)$$

The total turn off time is given by

$$t_{off} = t_{f-1} + t_{f-2} \quad (44)$$

The waveforms for phase A of the commutation period of the quasi-resonant converter are shown in Fig. 21. The simulation of the quasi-resonant converter is carried out in PSIM software. The single pulse mode operation is simulated here. The current through the resonant inductance and voltage across the resonant capacitor are shown in Fig. 22. The enlarge view of Fig. 22 is shown in Fig. 23. The

waveforms of the current through the resonant inductor and capacitor of Fig. 24 are the same as the waveforms shown in Fig. 20. The current through switch S1, S4 and diode D1 are shown in Fig. 25. The voltage across capacitor Cd and current through diode DA are also shown in Fig. 26. The value of current source is $I_o=30A$, the resonant inductor $L_r=5.4\mu H$, and resonant capacitor $C_r=0.5\mu F$. The excitation bus voltage $V_{dc}=312V$, the dump Capacitor $C_d=20\mu F$, and inductor $L_d=20mH$. $C_g=20\mu F$ and $R_g=20\Omega$.

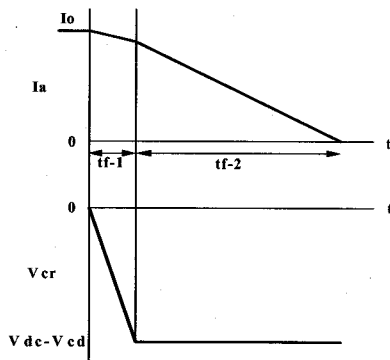


Fig. 21. Waveforms of phase A during commutation period.

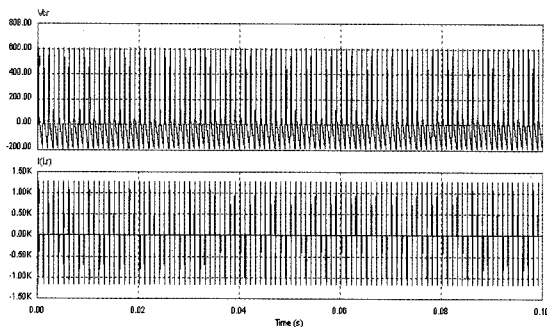


Fig. 22. Simulation results of I_{Lr1} and V_{cr1} .

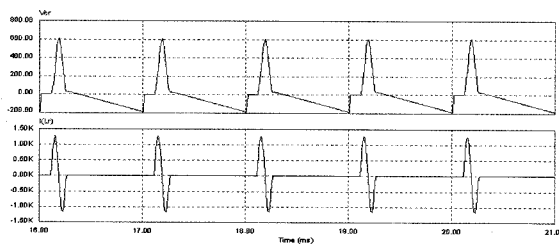


Fig. 23. Enlarge waveforms of I_{Lr1} and V_{cr1} .

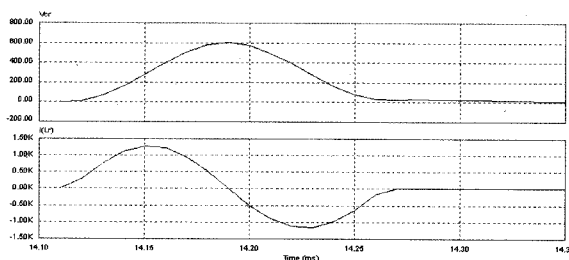


Fig. 24. Single cycle of I_{Lr1} and V_{cr1} .

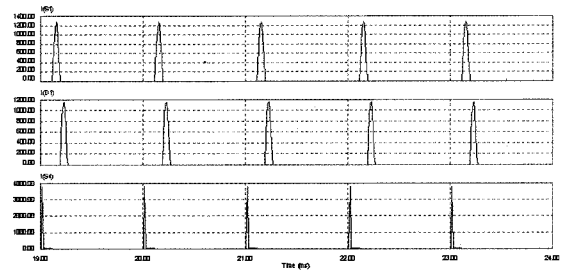


Fig. 25. Current through switch S1, S4, and D1.

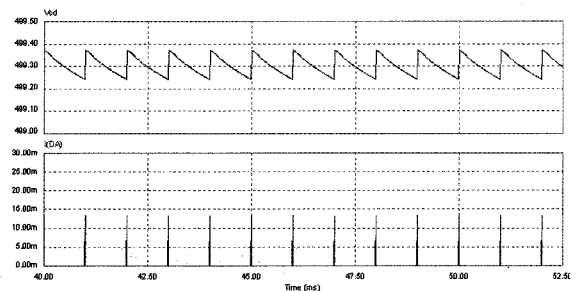


Fig. 26. Voltage across Cd and current through diode DA.

There is only one current sensor used in the quasi-resonant current controlled converter for the SRG. The sensor detects the sum of the currents in the two phases during the commutation from one phase to another. The regulator tends to maintain this sum constant. Therefore, the current in the ongoing phase is forced to follow the decreasing rate of the off going phase. The rise time and fall time of the phase currents are thus identical.

6. Comparison of Quasi-Resonant and Converters

Some of the advantages are common in both converters. Thyristors are used as power switches, which can withstand high voltage and current compared to IGBTs and MOSFETs. Therefore, the converters are suitable for high power applications. The large dump capacitor is used for energy recovery during the generating mode, which leads to reduction in fall time of the phase current during the commutation period. Thyristors are turned on and off at zero current. Therefore, the switching losses are reduced and efficiency is improved. However, the quasi-resonant converter has some disadvantages. During the active phase period, the current through the phase winding is assumed to be constant. To make the phase winding current constant, we assume that the speed of the machine is constant during the active phase, which is not the case in practice. During the commutation period, the current of the off going phase is decreased and the current in the in coming phase is increased. Yet, to make the current constant during the active phase period, the effect of the mutual inductance is

considered. This means that the rate of decrease of current in the off going phase is the same as the rate of increase of current in the on going phase. Therefore, the independent phase operation characteristic of SRM is no longer applicable with quasi-resonant converter. The control technique is less reliable compared to the resonant converter as well. This is because in quasi-resonant converter, only one current sensor is used due to the effect of the mutual inductance. However, in the SRM, the effect of mutual inductance is less compared to other machines. Therefore, some times the rate of decrease of the current in the off going phase is much higher than the rate of increase of the current of the on going phase. The total current sensed by the current sensor is the same even though the current in the on going phase is less. This may lead to malfunction of the control circuit. The resonant current controlled converter overcomes all the difficulty that we face in the quasi-resonant converter. In addition, due to the separate current sensors for each phase, the operation of each phase is independent of the other phases. Therefore, the resonant current converter is the most suitable for the high power applications.

7. Conclusion

The main features of the switched reluctance machines are low cost, simple construction, wide speed range operation, fault tolerance, and ability to withstand high temperatures. These advantages make SRG very popular compared to the induction and synchronous machines. One of the main concerns of this paper in SRG drives has been the converter design. The performance and the cost of the drive are highly affected by the converter switches. For very high power applications, IGBTs and MOSFETs are not suitable. MOSFETs with high voltage and high current capabilities are not even available. For IGBT-based converters, IGBTs need to be connected in parallel to be able to handle high currents. This considerably reduces efficiency and increases cost and complexity. Besides, maintaining balance current sharing between parallel IGBTs is of great concern. However, utilizing thyristors at very high power applications is feasible because of their high voltage and current capabilities. Yet, the main challenge in this work is that, to the best of our knowledge, thyristors have not been used for SRG applications. This is mainly because SRGs have traditionally been used for low power applications where IGBTs and MOSFETs are available.

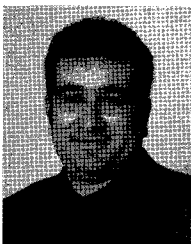
In this paper, novel thyristor-based resonant converters for high power switched reluctance generators have been proposed. Both turn-on and turn-off of the switches occur at zero current. Therefore, the switching losses are reduced

considerably. Active energy recovery into a high-voltage source is used to reduce the fall time of the phase current during commutation period. The proposed topologies have advantages of high efficiency and low stress on the switching devices. In addition, the resonant current controlled converter has advantages of simplicity on circuit configuration.

References

- [1] Y. P. Patel, "Thyristor-based resonant current controlled switched reluctance generator for distributed generation," M.S. Thesis, Illinois Institute of Technology, Chicago, IL, May 2003.
- [2] H. Broeck, D. Gerling, and E. Bolte, "Switched reluctance drive and PWM induction drive compared for low cost applications," in *Proc. 1993 European Conference on Power Electronics and Applications*, Sep. 1993, pp 71-76.
- [3] D. A. Torrey, "Variable-reluctance generators in wind-energy systems," in *Proc. 24th Annual IEEE Power Electronics Specialists Conference*, June 1993, pp. 561-567.
- [4] B. Fahimi, "On the suitability of switched reluctance drives for starter/generator application," in *Proc. IEEE 2002 Vehicular Technology Conference*, 2002, pp 2070-2075.
- [5] Radun, "Generation with the switched reluctance motor," in *Proc. IEEE 9th Applied Power Electronics Conference and Exposition*, 1994, pp. 41-47.
- [6] E. Mese, Y. Sozer, J. M. Kokernak, and D. A. Torrey, "Optimal excitation of a high speed switched reluctance generator," in *Proc. IEEE 15th Applied Power Electronics Conference and Exposition*, 2000, pp. 362-368.
- [7] Y. P. Patel and A. Emadi, "Suitability of switched reluctance machines in distributed generation systems," in *Proc. 2003 IASTED International Conference on Power and Energy Systems*, Palm Springs, CA, Feb. 2003.
- [8] D. A. Torrey, "Switched reluctance generators and their control," *IEEE Trans. on Industrial Electronics*, vol. 49, no. 1, pp. 3-14, Feb. 2002.
- [9] M. Barnes and C. Pollock, "Power electronic converters for switched reluctance drives," *IEEE Trans. on Power Electronics*, vol. 13, pp. 1100-1111, Nov. 1998.
- [10] S. Mir, "Classification of SRM converter topologies for automotive applications," *SAE 2002 World Congress*, Detroit, March 2000.
- [11] V. R. Stefanovic and S. Vukosavic, "SRM inverter topologies: a comparative evaluation," *IEEE Trans.*

- on *Industry Applications*, vol. 27, pp. 1034-1047, Nov./Dec. 1991.
- [12] B. Fahimi, G. Suresh, and M. Ehsani, "Large switched reluctance machines: a 1 MW case study," in *Proc. International Electric Machines and Drives Conference*, May 1999, pp. 84-86.
- [13] T. Uematsu and R. G. Hoft, "Resonant power electronic control of switched reluctance motor for electric vehicle propulsion," in *Proc. IEEE Power Electronics Specialists Conf.*, vol. 1, June 1995, pp. 264-269.
- [14] K.-D. Kim, D.-J. Shin, and U.-Y. Huh, "Application modified C-dump converter for industrial low voltage SRM," in *Proc. IEEE International Symposium on Industrial Electronics*, Pusan, South Korea, 2001, pp. 1804-1809.
- [15] R. Krishnan and S. Lee, "Analysis and design of a single switch per phase converter for switched reluctance motor drives," in *Proc. 25th Annual IEEE Power Electronics Specialists Conference*, June 1994, pp. 485-492.



Ali Emadi

He is a professor of electrical engineering and the director of the Electric Power and Power Electronics Center at Illinois Institute of Technology (IIT), where he has established research and teaching facilities as well as courses in power electronics, motor drives, and vehicular power systems. Dr. Emadi is the founder, director, and chairman of the board of the Industry/Multi-university Consortium on Advanced Automotive Systems (IMCAAS). He is also the founder and Chief Technology Officer (CTO) of Hybrid Electric Vehicle Technologies, Inc.

Dr. Emadi is the recipient of numerous awards and recognitions. He has been named the Eta Kappa Nu Outstanding Young Electrical Engineer of the Year 2003 by virtue of his outstanding contributions to hybrid electric vehicle conversion. He also received the 2005 Richard M. Bass Outstanding Young Power Electronics Engineer Award from the IEEE Power Electronics Society. Dr. Emadi is the recipient of the 2002 University Excellence in Teaching Award from IIT as well as the 2004 Sigma Xi/IIT Award for Excellence in University Research. He directed a team of students to design and build a novel motor drive, which won the First Place Overall Award of the 2003 IEEE/DOE/DOD International Future Energy Challenge for Motor Competition.

Dr. Emadi was the General Chair of the 2005 IEEE Vehicle Power and Propulsion and SAE Future Transportation Technology Joint Conference. Dr. Emadi is the author/co-author of over 200 journal and conference papers as well as several books including *Vehicular Electric Power Systems* (Marcel Dekker, 2003), *Energy Efficient Electric Motors* (Marcel Dekker, 2004), *Uninterruptible Power Supplies and Active Filters* (CRC Press, 2004), and *Modern Electric, Hybrid Electric, and Fuel Cell Vehicles* (CRC Press, 2004). He is also the editor of the *Handbook of Automotive Power Electronics and Motor Drives* (Marcel Dekker, 2005).



Yogesh P. Patel

He received the B.S. degree in Electrical Engineering from Maharaja Sayajirao University of Baroda, Baroda, India and M.S. degree in Electrical Engineering from Illinois Institute of Technology, Chicago. From 2001 to 2003, he was with Grainger Power Electronics Laboratory, Illinois Institute of Technology, as Research Assistant. From 2003 to 2005, he was with APL Engineered Materials Inc (Division of Advance Lighting Technology), Urbana, IL as an Electrical Engineer. Since 2005, he has been at Spellman High Voltage Electronics Corp. Hauppauge, NY, as Electrical Engineer. His research interests are in the area of adjustable speed drives and power electronics converters for switched reluctance machines.



Babak Fahimi

He received his PhD in Electrical Engineering from Texas A&M University, College Station in 1999. Currently he is with the department of electrical engineering at University of Texas-Arlington as an assistant professor. His areas of interest include microscopic analysis of electromechanical energy conversion, digital control of adjustable speed motor drives, and design and development of power electronic converters. Dr. Fahimi is the recipient of IEEE Richard M. Bass young power electronics investigator award from power electronics society and office of naval research young investigator award.